7

Interactions and Transitions in Imidazolium Cation Based Ionic Liquids

Madhulata Shukla, Nitin Srivastava and Satyen Saha
Department of Chemistry, Faculty of Science
Banaras Hindu University Varanasi
India

1. Introduction

Ionic liquids (ILs) raise considerable research interest not only as promising new solvents for the replacement of conventional solvents in synthesis, but also as new liquid materials.[1-2] It appears from the recent breakthroughs that the novel properties of various ILs are of more interest than mere application as 'green solvent' in traditional organic chemistry. ILs are now rediscovered to be whole new materials with many wonderful properties, much of it are yet to be discovered. The defining characteristic of ILs is of their constitutions - molecular ions as their building blocks as opposed to molecules in the traditional solvents. In other words, ILs or molten salts in general are defined as liquids composed of ions only, either at room temperature or at elevated temperatures (below 100°C). ILs are rather unique in the sense that in addition to ionic and covalent interactions, there are relatively weaker interactions such as H-bondings, and π-stacking, which are not commonly found in conventional solvents.[3-4] The nature of the forces in different ILs may however differ from one another and mainly control their physical properties. As the properties of any material depends on the structure of molecules in different phases, it is very important to understand the structural features of ILs in depth. Researchers have paid considerable attention towards pyridinium, imidazolium and pyrrolidinium based ILs in addition to ammonium and phosphonium ILs. Pyridinium based ILs are heterocyclic aromatic compounds proven to have great potential in organic synthesis and biocatalyst. Compared with the imidazolium based ILs, few studies have examined the biodegradability of pyridinium based ones.[5] Due to biodegradable property of these pyridinium and pyrrolidinium ILs, it has been extensively studied.[6-12] On the other hand, pyrrolidinium ILs are mainly involved in dye sensitized solar cell and batteries.[11] Since structure plays the vital role for any application, recently detailed x-ray scattering studies have been reported on the pyrrolidinium cations based ILs while varying the length of the alkyl chain attached with the ring.[12] Interestingly, diffraction pattern shows signature of intermediate range ordering similar to that of in imidazolium based ILs. Among all ionic liquids, imidazolium cation based ILs are the most extensively studied ILs, and therefore our discussion will mainly be confined with imidazolium cation based ILs.

As of true 'designer solvent', it has been observed that a small variation in imidazolium cation (such as increase or decrease in alkyl chain length) alters their physical properties

(melting point, viscosity, conductivity etc.) drastically.[13-14] For instance, density of IL decreases as the length of the alkyl chain on the cation increases up to a certain length. For a given cation, the density increases as the molecular weight of the anion increases. Many of ILs tend to subcool easily, forming glasses at very low temperature rather than exhibiting crystallization or melting transitions. The thermal stability increases with increasing anion size, and heat capacities increases with temperature and increasing number of atoms in IL.[15] The work reported by Anderson et. al. [16] uses a linear free energy approach to characterize different imidazolium and pyridinium based Room temperature ionic liquids (RTILs) on the basis of their distinct multiple solvation interactions with probe solute molecules. This model provides data that can be used to identify the interactions and properties that are important for specific chemical applications. It has also been shown that the anion has greater effect on hydrogen bond basisity of RTIL while the effect of the cation was generally found to be small. RTILs found to exhibit multiple behaviour such that it acts as polar solvents in organic reactions containing polar molecules and acts as less polar solvents in the presence of less polar molecules.[16] Hence study of interactions present between cation and anion as well as with probe molecules in ILs are very important. To get more insight of interactions presents in ILs, theoretical calculations are found to be of great help.[17-20] Density Functional Theory (DFT) is a quantum mechanical theory used in physics and chemistry to investigate the electronic structure (mainly in ground state) and sometime used to calculate various thermodynamic properties of a molecule. With this theory, the property of many-electron system can be determined by using functional i.e. function of another function (electron density). At present DFT is the most popular and a versatile method available in computational chemistry.[21-23] Our work with DFT is mainly on the structural investigation of ILs as most of them are liquids at room temperature, so their structural investigations are very difficult by conventional techniques like single crystal x-ray diffraction (SCXRD). Hence DFT calculation found to be of great useful in predicting the molecular structure, as well as interactions present in a given molecule.[4, 21] Magnetic moment, dipole moment and many other physical properties of a molecule can also be calculated by the same. In addition, the calculated vibrational frequency (both IR and Raman) of the molecule gives us a strong base to analyze the experimental spectra and also the effect of interaction causing shifting in IR bands. Chang et. al have described using DFT that how the cation-anion interaction lead to shifting in vibrational frequencies.[24] Hence theoretical calculation found to be of great valuable in explaining the interactions present in a given IL.

Here we have addressed the following very specific issues related to important class of imidazolium cation based ILs. It has been found that with variation of anion, cation being the same, physical state of ILs changes drastically.[25] **1**) For example, while bmimCl and bmimBr found to be solid at room temperature [4,21] whereas bmimI is liquid at room temperature [bmim:1-butyl-3-methylimidazolium].[26] We have studied the structural features of these ILs by DFT calculation which found to predict the ILs structures quite well. Further it has been found that in $bmimBF_4$, $bmimPF_6$ and $bmimNTf_2$ multiple H-bondings were found between cation and anion at a specific orientation [18,27], whereas in bmimCl, bmimBr and bmimI, only one predominant H-bonding was found to exist. It is proved that H-bonding found to play crucial role in describing the physical state of different ILs.[21-22,24] In this chapter we have also addressed the colour of ionic liquids which is due to the transition in the visible wavelength range. While the chloride and bromide analogues (i.e., bmimCl and bmimBr) are colourless, the corresponding iodide salt is found to be

coloured.[23,26] The colour issue is important since during the synthesis of these derivatives (e.g., halogen and PF_6, BF_4 anion containing alkylimidazolium ILs), often impurity imparts colour making it difficult to understand whether the colour is inherent to ILs concerned or is due to the colour impurity.[28-29] Especially, from spectroscopic application point of view it is very important to have optically transparent windows of the ILs.[28-30] TD-DFT theoretical calculation found to play a crucial role to explain, whether colour of given IL is intrinsic or due to impurity present in it.

2. Experimental

2.1 Synthesis of 1-butyl-3-methylimidazolium halide (bmimX, where X^-= Cl, Br, I, NTf_2 , PF_6 and BF_4)

Synthesis of all bmimX have been done following the reported method [4,23,31] with some modifications to get the product as much pure as possible. The major modification is mainly of the temperature at which reactions were done. Since we have used considerable less temperature than generally reported, the time required for the reactions are also much higher. Nevertheless, this low temperature reaction has been found to provide much pure ILs.

2.1.1 Synthesis of bmimCl

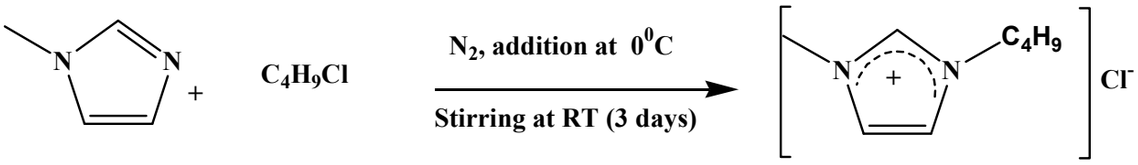

N-methylimidazole was dissolved in required amount of dry acetonitrile followed by slow addition of butyl halide at 0^0C with constant stirring under N_2 atmosphere in dark. The solution was left at 0^0C for 2h and then stirred for 3 days while keeping the temperature below 40^0C. The progress of the reaction was monitored by checking the TLC (removal of methylimidazole). Acetonitrile (ACN) was then evaporated at reduced pressure at the same temperature. Pale yellow colour viscous liquid was obtained (yield: 70%) which was then washed with dry ethyl acetate and then followed by dry diethyl ether. During washing bmimCl was solidified. bmimCl was further purified with activated charcoal to remove coloured impurities. Finally, it was kept under reduced pressure (10^{-3} bar) for 5 h at 40^0C. Precautions were taken to eliminate the presence of water or organic solvents in the purified IL. The product was confirmed by IR: 754 cm^{-1}, 1168 cm^{-1}, 1463 cm^{-1}, 1571 cm^{-1}, 1628 cm^{-1}, 2870 cm^{-1}, 2960 cm^{-1}, 3098 $cm^{-1}$and 3152 cm^{-1} and ^{1}H NMR, (in $CDCl_3$, ppm); 0.93(t), 1.36(sextet), 1.84(q), 4.11(s), 4.31(t), 7.50(s), 7.65(s), 10.38(s).

2.1.2 Synthesis of bmimBr

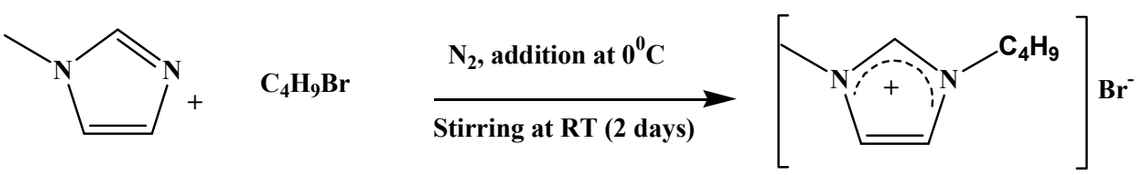

Following the above mentioned procedure, bmimBr was synthesized. Here stirring was carried out for 2 days. The pale yellow coloured solid was obtained which was further treated with activated charcoal to remove coloured impurities. Thus obtained bmimBr was kept under reduced pressure (10^{-3} bar) for 5 h at 40^0C. Precautions were taken to eliminate the presence of water or organic solvents in the purified IL. The product was confirmed by IR: 794 cm^{-1}, 1168 cm^{-1}, 1463 cm^{-1}, 1570 cm^{-1}, 1629 cm^{-1}, 2871 cm^{-1}, 2960 cm^{-1}, 3086 $cm^{-1}$and 3155 cm^{-1} and ^{1}H NMR, (in $CDCl_3$, ppm); 0.94(t), 1.35(sextet), 1.86(q), 4.13(s), 4.31(t), 7.39(s), 7.49(s), 10.35(s).

2.1.3 Synthesis of bmiml

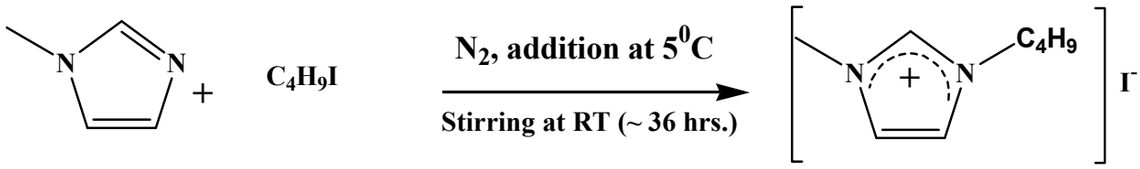

Above reported procedure was also followed to synthesize the bmimI. Pale yellow colour viscous liquid was obtained (yield: 94%) which was then washed with dry ethyl acetate and dry diethyl ether. The pale yellow coloured IL thus obtained was kept under reduced pressure (10^{-3} bar) for 5 h at 40 ^{0}C. Precautions were taken to eliminate the presence of water or organic solvents in the purified IL. The purity of product was confirmed by IR: 752 cm^{-1}, 1167 cm^{-1}, 1461 cm^{-1}, 1568 cm^{-1}, 1628 cm^{-1}, 2870 cm^{-1}, 2958 cm^{-1}, 3098 $cm^{-1}$and 3138 cm^{-1} and ^{1}H NMR, (in $CDCl_3$, ppm); 0.95(t), 1.39(sextet), 1.90(q), 4.13(s), 4.35(t), 7.53(s), 7.61(s), 9.95(s).

2.1.4 Synthesis of bmimNTf_2

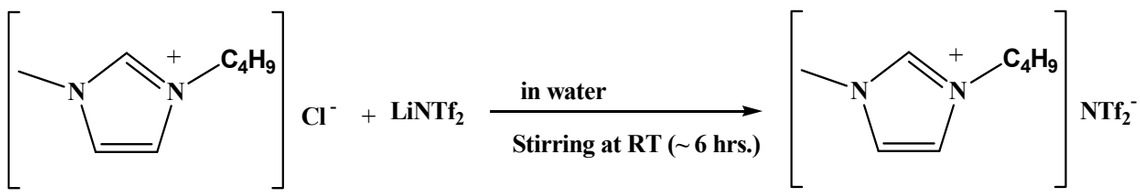

bmimNTf_2 was synthesised from bmimCl (7g, 43mmol) which was dissolved in 5 mL of triple distilled water followed by the slow addition of $LiNTf_2$ solution (13g, 47mmol in 13 mL triple distilled water) with stirring. After addition of $LiNTf_2$ solution in bmimCl solution, colour of solution changes to milky white and two layers were separated and the reaction mixture was stirred for further 6 hrs. Whole reaction mixture was then transferred in to a separating funnel and bmimNTf_2 was extracted with DCM. Then DCM layer was washed with cold water for removal of chloride ion which was monitored with the help of aqueous acidified solution of $AgNO_3$. DCM solution was dried over anhydrous $MgSO_4$ and then the dried DCM was evaporated providing colourless liquid which was kept under vacuum for removal of solvent and other volatile impurities. (yield: 85%) This was further treated with activated charcoal and then passed through column containing alumina and celite to remove coloured impurities. Precautions were taken to eliminate the presence of water or organic solvents in the purified IL. The product was confirmed by IR: 744 cm^{-1}, 845 cm^{-1}, 1057cm^{-1}, 1140 cm^{-1}, 1194 cm^{-1}, 1350cm^{-1}, 1464 cm^{-1}, 1573 cm^{-1}, 2937 cm^{-1}, 2964 cm^{-1}, and 3161 cm^{-1} and ^{1}H NMR, (in $CDCl_3$, ppm); 0.93(t), 1.32(sextet), 1.79(q), 3.93(s), 4.14(t), 7.26(s), 7.31(s), 8.73(s).

2.1.5 Synthesis of $bmimPF_6$

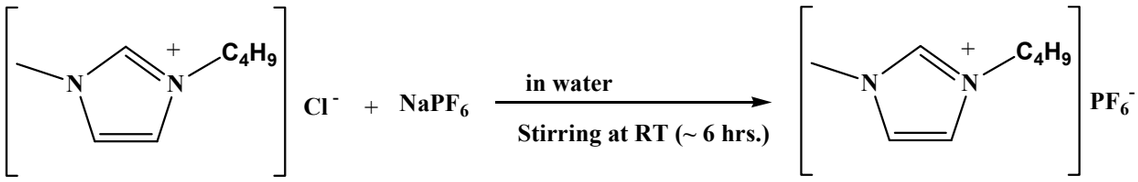

Above procedure reported for synthesis of $bmimNTf_2$ was followed for synthesizing $bmimPF_6$ also. Here instead of $LiNTf_2$, $NaPF_6$ was added to bmimCl solution. Yield was found to be 86%. The product was confirmed by IR: 748 cm^{-1}, 839 cm^{-1}(P-F stretching), 1112 cm^{-1}, 1164 cm^{-1}, 1464 cm^{-1}, 1573 cm^{-1}, , 2876 cm^{-1}, 2965 cm^{-1} and 3169 cm^{-1} and ^1H NMR, (in $CDCl_3$, ppm); 0.94(t), 1.23(sextet), 1.75(q), 3.94(s), 4.05(t), 7.26(s), 7.29(s), 8.33(s).

2.1.6 Synthesis of $bmimBF_4$

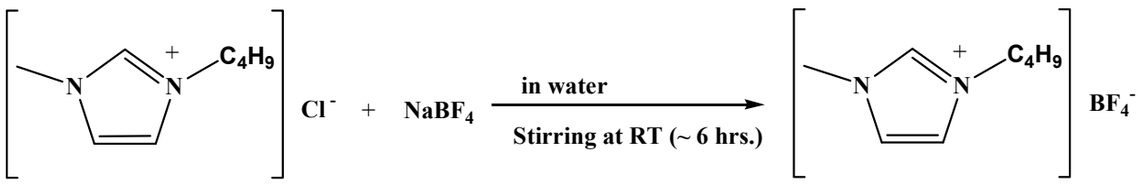

For synthesis of $bmimBF_4$ above mentioned procedure was followed, except that $NaBF_4$ was added instead of $LiNTf_2$. Yield of the product was found to be 80% Precautions were taken to eliminate the presence of water or organic solvents in the purified IL. The product was confirmed by IR: 757 cm^{-1}, 849 cm^{-1}, 1053cm^{-1} (B-F stretching), 1169 cm^{-1}, 1464 cm^{-1}, 1573 cm^{-1}, 1625 cm^{-1}, 2876 cm^{-1}, 2963 cm^{-1}, 3121 cm^{-1} and 3162 cm^{-1} and ^1H NMR, (in $CDCl_3$, ppm); 0.85(t), 1.29(sextet), 1.81(q), 3.89(s), 4.15(t), 7.33(s), 7.41(s), 8.82(s).

3. Computational method

The Gaussian 03 program [32] was used for the Density Functional Theory (DFT) calculation of different ILs. The basis sets already implemented in the program were used for the different types of calculations. The geometries of isolated ion pairs of ILs were optimized at the Becke's three parameter hybrid method with LYP correlation (i.e. B3LYP).[33] While 6-31G++(d,p) basis set was used for C, H, N, O, S, F and P, DGDZVP basis set was used for I atom.[34] Due to large atomic number of iodine atom, 6-31 G++(d,p) basis set is found to be incapable of predicting accurate structure and vibrational spectrum of bmimI. Optimisation, frequency calculation and Time-Dependent Density functional Theory (TD-DFT) were also performed at the B3LYP level of calculation. The absence of imaginary vibrational frequencies in vibrational spectrum ensures the presence of a true minimum.

4. Results and discussion

4.1 Studies of interactions by single crystal x-ray diffraction and Raman spectroscopic techniques

Among all imidazolium cation based ILs mentioned above, bmimCl and bmimBr are the two prototype ILs that have been studied extensively. [4, 21, 31] The interesting aspects which make these two monoatomic anion based ILs well studied is their existence both in

solid and super cooled liquid phases. Therefore these two ILs give the opportunity to study the structures and interactions present in both solid and liquid state with a possibility to make a correlation. Crystal structures of bmimCl and bmimBr at room temperature have been well studied.[4,21,31] It has been discovered simultaneously and independently by,

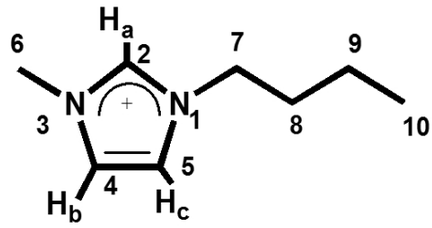

Fig. 1. Schematic representation of bmim catiom [bmim: 1-butyl-3-methylimidazolium]

Saha et. al. [4] and Holbrey et. al.[31] that bmimCl crystal shows two crystal polymorphism. Schematic diagram of bmim cation has been presented in Figure 1. In crystal 1 (Figure 2a), the *n*-butyl group takes *trans-trans* (**TT**) conformation with respect to C_7-C_8 and C_8-C_9 bonds, while in crystal 2 (Figure 2b), n-butyl group takes *gauche-trans* (**GT**) conformation with respect to C_7-C_8 and C_8-C_9 bonds similar to that of bmimBr conformation.[4, 25] Powdered x-ray diffraction patterns of the two polymorphs of bmimCl and bmimBr was recorded and found that the pattern for crystal 2 and bmimBr somewhat resembles each other, while that of bmimCl crystal 1 is distinct from the other two.[4,21]

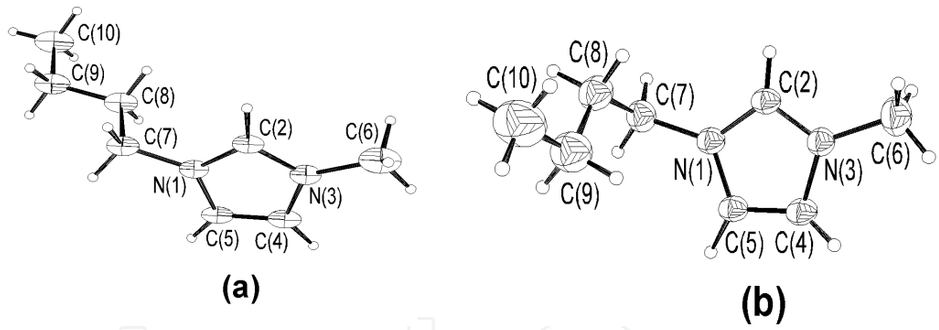

Fig. 2. The structure of bmim cation in bmimCl. (a) n-butyl chain has *trans-trans* conformation with respect to C7-C8 and C8-C9 bonds and therefore described as Crystal 1 or TT in text. (b) The crystal structure of bmim cation in bmimBr. In this case, n-butyl chain has *gauche-trans* conformation with respect to C7-C8 and C8-C9 bond and therefore termed as GT or Crystal 2 in the text.

Presence of polymorphs is found to be due to the different interactions in the crystal systems. In crystal 1, a couple of bmim cations form a pair through a *hydrophobic interaction* among stretched n-butyl group. Those pairs stack together and form a column in which all imidazolium ring planes are parallel with one another. Two types of cation columns with different orientations exist. Hamaguchi and co-workers have been studied these ILs extensively by Raman spectroscopic techniques.[21] It was found that Raman spectra of two polymorphs are markedly different from each other. In the wavenumber region 600-700 cm^{-1}, where ring deformation bands are expected, two bands appear at 730 cm^{-1} and 625 cm^{-1} in bmimCl crystal 1 (i.e., **TT** conformation), while another couple of bands appear at 701 and 603

cm^{-1} in bmimCl crystal 2 (**GT**) and bmimBr but not in bmimCl crystal 1. In order to clarify the origin of these bands, Ozawa et. al. has done extensive DFT calculation on these Ils.[22] It shows that the 625 cm^{-1} band of bmimCl crystal 1 and the 603 cm^{-1} band of bmimBr originates from the same ring but have different magnitude of couplings with the CH_2 rocking vibration of the C_7 carbon. The coupling occurs more effectively for the *gauche* conformation around the C_7-C_8 bond, resulting in a lower frequency in the GT form (603 cm^{-1}) than in the TT form (625 cm^{-1}). It was noted that the coupling with the CH_2 rocking mode having a higher frequency pushes down the frequency of the ring deformation vibration. The same coupling scheme holds for another ring deformation mode and the GT form has a lower frequency (701 cm^{-1}) than the TT form (730 cm^{-1}). It is therefore elucidated from the DFT calculation that the 625 and 730 cm^{-1} bands are the characteristics of the *trans* conformation around the C_7-C_8 bond, while the 603 and 701 cm^{-1} bands are the characteristics of the *gauche* conformation. In other words, one can use these bands as key bands to probe the conformation around the C_7-C_8 bond of the bmim cation. The 500 cm^{-1} band of the bmimBr is ascribed to the C_7-C_8-C_9 deformation vibration of the *gauche* conformation around the C_7-C_8 bond. The Raman spectra of all *liquid* bmimX (where X= Cl, Br, I, BF_4, PF_6) found to be similar, suggesting that bmim cation is similar for all these liquids. Both the two sets of marker bands, 625 and 730 cm^{-1} for the *trans* conformation and the 603 and 701 cm^{-1} band for the *gauche* conformation appears in all the liquid spectra. Therefore, at least two rotational isomers, one having a *trans* conformation and other having *gauche* conformation around the C_7-C_8 bond co-exist in liquid bmimX. The physical properties of these two polymorphs are found to be different, e.g., the melting point of crystal 1 is 41^0C while that of crystal 2 is 66^0C. Different melting points are due to different types of interactions present in the system which is further due to the different kind of molecular conformations (e.g., TT, GT etc.).

4.2 Studies of interaction through ^{1}HNMR

NMR data clearly explain the strength of interaction between cation and anion. Figure 3 shows ^{1}HNMR spectra of bmimX. C_2-H proton shiftings were recorded to be 10.38ppm,

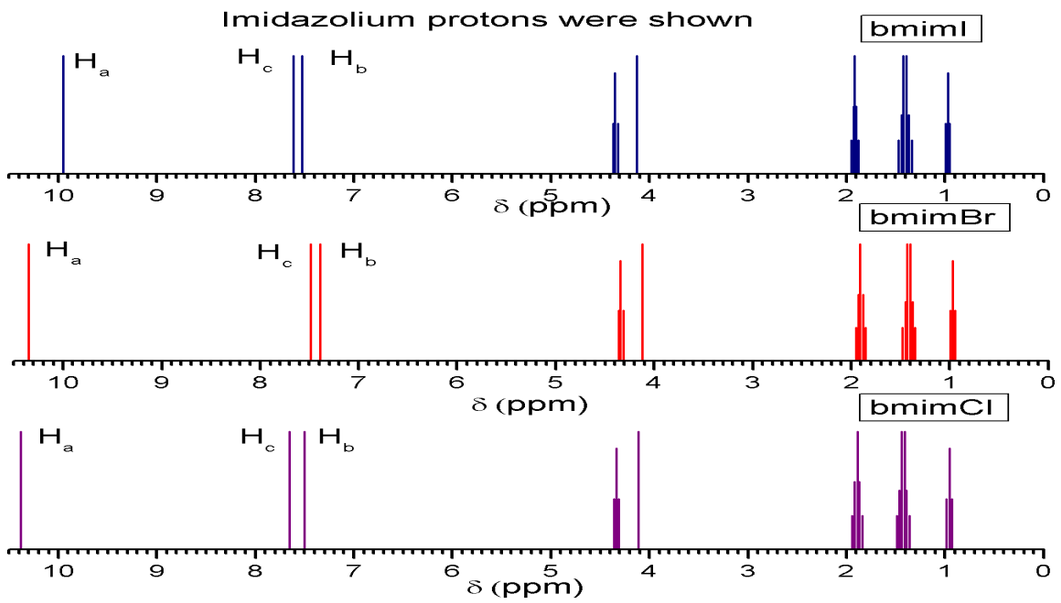

Fig. 3. ^{1}HNMR shift of 1-butyl-3-methylimidazolium (bmim) cation with various halide anions.

10.35ppm, 9.95ppm in bmimCl, bmimBr and bmimI respectively, explaining that H-X interaction is strongest in bmimCl and then in bmimBr and least in bmimI. When these values compared with the bmimNT_2, bmimBF_4 and bmimPF_6, this shift was found to be 8.73 ppm, 8.82 ppm and 8.33 ppm respectively, explaining that interaction between C_2-H and anion in these ILs is weak when compared with bmimCl, bmimBr and bmimI. Variation of IR spectra which is discussed later in this chapter have been found to be nicely correlated with the NMR studies of these ILs.

4.3 Study of interactions in molecular structure of different ILs using DFT calculations

The optimized molecular structure of bmimX (where X= Cl, Br, I, PF_6, BF_4 and NTf_2) determined at B3LYP/6-31G++(d,p) level of computation (except DGDZVP basis set used for I atom) are shown in **Figure 4(a-f)**

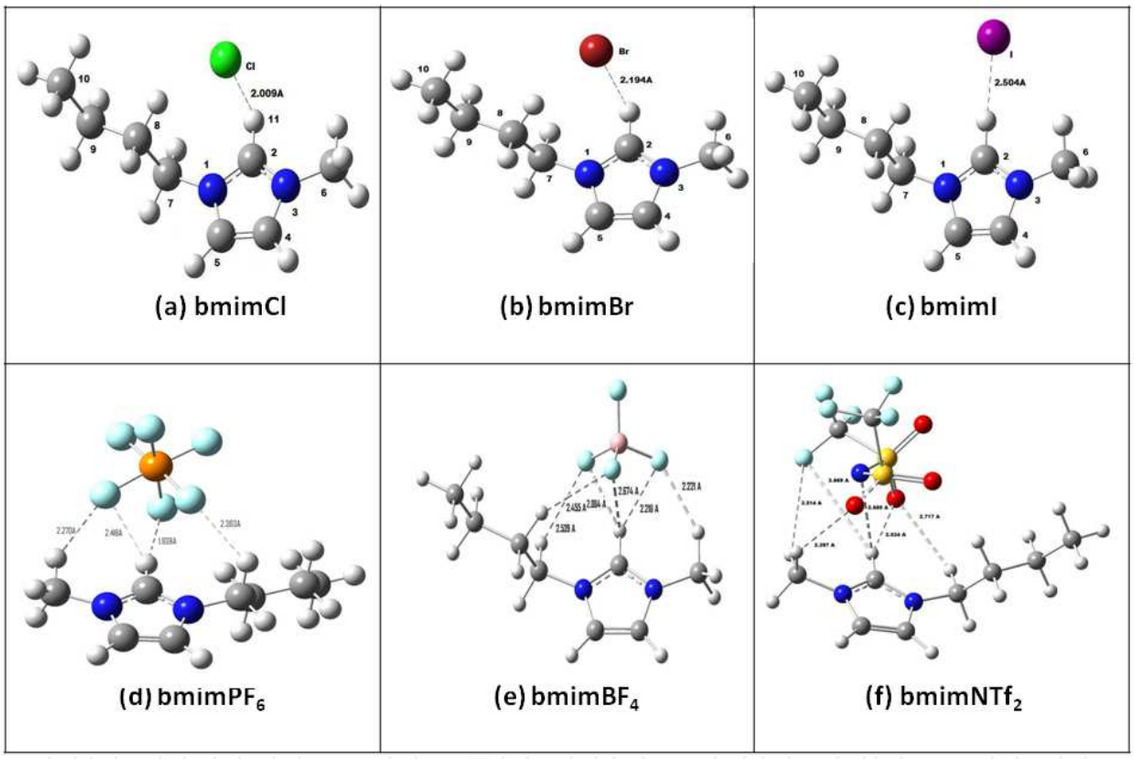

Fig. 4. DFT optimized structure of different imidazolium based Ils in gas Phase

The optimized structures reveal that the imidazolium ring is a planar pentagon as expected. The average bond length of 1.34 Å for the N1-C2 and C2-N3 in all the three ILs indicates the nature of conjugated double bond character. Further N1-C5 and N3-C4 bond lengths are (1.38 Å) shorter than a pure C-N single bond (1.47 Å). Bond length of C4-C5 is in the range of normal C=C bond (1.33 Å). It can be seen from the **Table 1** that dihedral angles (~180^0) of the butyl group explain the *trans* conformations in all 1-butyl-3-methyl-imidazolium halide ILs studied. Similar observation was observed for bmimPF_6, bmimBF_4 and bmimNTf_2 ILs. While the C^2-H-----X distance increases gradually from Cl^- to I^- following the trend of electronegativity (Cl^-=3.0, Br^-=2.8, I^-=2.5), the bond angle also decreases gradually from bmimCl to bmimI. The C_2-H---Cl interaction is thus found to be the strongest among all and

the order was found to be C_2 –H----Cl > C_2- H----Br > C_2-H---I. Further the position of anion was found to be crucial in determining whether an IL will be liquid at ambient temperature or not. As mentioned earlier that bmimI exist in liquid state (m.p.–72°C) whereas its corresponding chloride, (bmimCl) and bromide (bmimBr) ILs are solids at 20°C. As mentioned earlier, melting point of bmimCl are 41°C and 66°C depending on the type of crystal polymorph, while that of bmimBr is 79°C.[21] From our calculations it is observed that while Cl^- and Br^- ions are present in the plane of the imidazolium ring, position of iodide anion is found to be below or above the plane.[23,34] The position of Cl^- and Br^- are satisfactorily matching with what was found in single crystal x-ray diffraction data. [21] This led us to conclude that because of the small size of the Cl^- and Br^-, there is compact packing of ions in the crystal lattice leading to higher melting points. Due to the large size of iodide anion, it does not fit well in the lattice. This makes it difficult to have close packing leading to liquid state at ambient temperature. It is important to mention here that in addition to ion size, interionic interactions also play major role in determining the state of an IL. Further, various dihedral angles of type <N_1-C_2-H-X (see **Table 1**) also indicates that the Cl^- and Br^- anions are in the plane of the imidazolium ring whereas I^- ion is out of plane.[17]

Parameters	bmimCl	bmimBr	bmimI
C_2-H	1.12 Å	1.11 Å	1.09 Å
C^2H---X	2.01 Å	2.19 Å	2.50 Å
C_2-N_1	1.34 Å	1.34 Å	1.34 Å
C_2-N_3	1.34 Å	1.34 Å	1.34 Å
N_1-C_5	1.38 Å	1.38 Å	1.38 Å
N_3-C_4	1.38 Å	1.38 Å	1.38 Å
C_4-C_5	1.36 Å	1.36 Å	1.36 Å
N_3-C_6	1.46 Å	1.46 Å	1.46 Å
<N-C-N	108.4^0	108.4^0	108.4^0
<C-H-X	158.8^0	153.7^0	143.4^0
<C_7-C_8-C_9-C_{10}	178.9^0	177.8^0	179.9^0

Table 1. Selected bond lengths, bond angles and dihedral angles as obtained from DFT calculation.

From **Figure 4(a-f)** it is clear that in bmimCl, bmimBr and bmimI, only one H-bonding was found with C_2-H, in a specific orientation whereas in case of BF_4, PF_6 and NTf_2 based imidazolium ILs multiple H-hydrogen bonding are seen. While in bmimCl, bmimBr and bmimI, C_2-H---X distances were found to be 2.01 Å, 2.19 Å and 2.50 Å respectively, in case of bmimPF_6, H----F distance was found to be 2.418 Å, 1.93 Å, 2.27 Å and 2.36 Å, in bmimBF_4, H----F distance found to be 2.53 Å, 2.45 Å, 2.21 Å and 2.08 Å and in bmimNTf_2, in addition to H---F distance (3.51 Å and 3.66 Å) O-H distance found to be 2.03 Å, 2.39 Å and 2.71 Å. Further in addition to the C2-H hydrogen bonding, C4-H and C5-H also participate in H-bonding interaction with halide anion but stabilization due to H-bonding interaction between cation and anion is found to be more in case of interaction involving C2-H compared to that of involving C4 and C5-H. [35] It is because, while C2 is positive (due to the electron deficient π bond formation of C=N bond), the C4 and C5 are essentially neutral (due to π bond formation between two carbon sharing equally the available electrons). [36]

4.4 Calculated vibrational spectra, analysis and its correlation with experiment

Vibrational spectra of all the ILs has been calculated at same level of calculation and using the same basis set in gas phase. The calculated vibrational spectra for bmimCl, bmimBr and bmimI have been shown in **Figure 5** and the spectral bands with the corresponding assignments are presented in **Table 2**. Vibrational frequencies corresponding to different vibrational motions such as stretching, in plane bending (*ip*) out of plane bending (*op*), wagging, rocking etc were assigned based on the predominant motion of the atoms and magnitude of the displacement vector associated with the atoms involved in concerned vibration. Most of the assignments were found to be matching with the literature values of similar compounds.[27] It is interesting to note that wavenumber for most of the motions for bmimCl and bmimBr are nearly same, but differs considerably for the same motion in bmimI. Among all, the most prominent and interesting observation is the shift of C_2-H stretching band in different ILs studied. While the band appears at 2652 cm^{-1} for bmimCl, 126 cm^{-1} blue shift is observed for the same in bmimBr. A further blue shift of 212 cm^{-1} is observed in bmimI (i.e., appears at 2990 cm^{-1}).

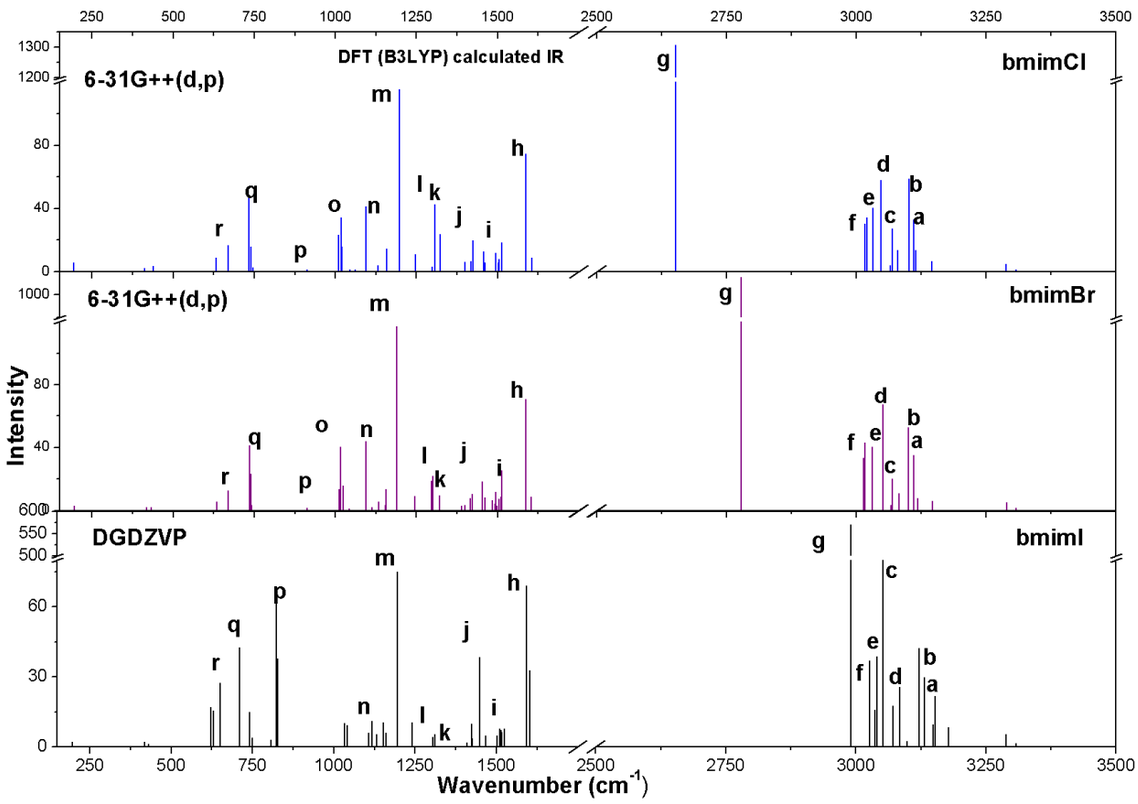

Fig. 5. DFT calculated IR spectra of bmimX where X=Cl^-, Br^-, I^-indicating the blue shift of the C_2-H stretching band (g) with different anions.

This can be explained considering the fact that this hydrogen participates in hydrogen bond formation with the halide anion. Since the strength of hydrogen bond depends on the type of anion (mainly on its electronegativity), shift in frequencies were observed.

Bands	Wavenumber /cm^{-1}			Assignment of bands
	bmimCl	bmimBr	bmimI	
a	3110	3110	3132	Asym. stretching of terminal CH_3 group
b	3101	3100	3121	Asym. stretching of C-H bond in butyl group
c	3069	3070	3052	Sym. stretching of C-H in N-CH_3
d	3048	3051	3084	Sym. stretching of C-H in N-CH_2
e	3032	3031	3040	Sym. stretching of C-H in terminal CH_3 group
f	3016	3016	3027	Sym. stretching of H-C-H in butyl group
g	2652	2778	2990	stretching of C_2-H bond
h	1588	1587	1593	*ip* bending of im. ring
i	1514	1513	1517	Scissoring of H-C-H in butyl group
j	1424	1423	1424	Wagging of H-C-H in butyl group
k	1323	1322	1327	Rocking of H-C-H in butyl group
l	1307	1300	1304	*ip* bend of im ring
m	1198	1190	1198	*ip* bend of im ring, CCCC str
n	1095	1094	1118	stretching of C-N(CH_3) & bending in N-CH_3
o	1019	1017	-	*op*. bend of C_2-H
p	841	844	827	Rocking in H-C=C-H ring
q	734	739	710	Wagging of HC=CH
r	669	671	651	*op* bending of im. ring

Where sym- symmetric, asym- asymmetric, ip- inplane, op- out of plane

Table 2. Selected DFT calculated harmonic vibrational frequencies for bmimX ILs in gas phase and their band assignment.

In other word, this shift in C_2-H stretching frequency is an indicator of the strength of the hydrogen bond which is formed between C_2-H and halide anion. These data suggests that the hydrogen bonding is strongest in case of bmimCl and weakest in bmimI.[23] This observation is exactly matching with the finding of ^{1}H NMR results asdiscussed earlier in this chapter. Further the single crystal X-ray crystallographic data that are available for bmimCl and bmimBr also corroborate with our results discussed here.[4,17,25] In addition, as expected, the position of the band arising due to 'out of plane' bending motion of C_2-H is also sensitive to the type of anion. Interestingly the I^- is found to be present out of plane of imidazolium ring which restricts the out of plane bending of C_2-H bond, making it absent in the IR spectrum whereas band at 1019 cm^{-1} in bmimCl and 1017 cm^{-1} in bmimBr are due to out of plane bending of C_2-H bond. Hence in bmimCl and bmimBr, Cl^- and Br^- found to exist in plane of imidazole ring and hence provide strong hydrogen bonding with C_2-H and therefore found to exist in solid state. Whereas in case of bmimI, I^- is present out of plane thus providing less interaction with C_2-H and therefore found to exist in liquid state.[23] Infrared (IR) spectrum of synthesised bmimI is compared with the calculated one and is presented in **Figure 6**. The overall correlation of band positions in calculated vibrational frequencies agrees reasonably well with that obtained experimentally. Hence, it appears thatB3LYP level of calculation gives reasonably good correlation between the experimental

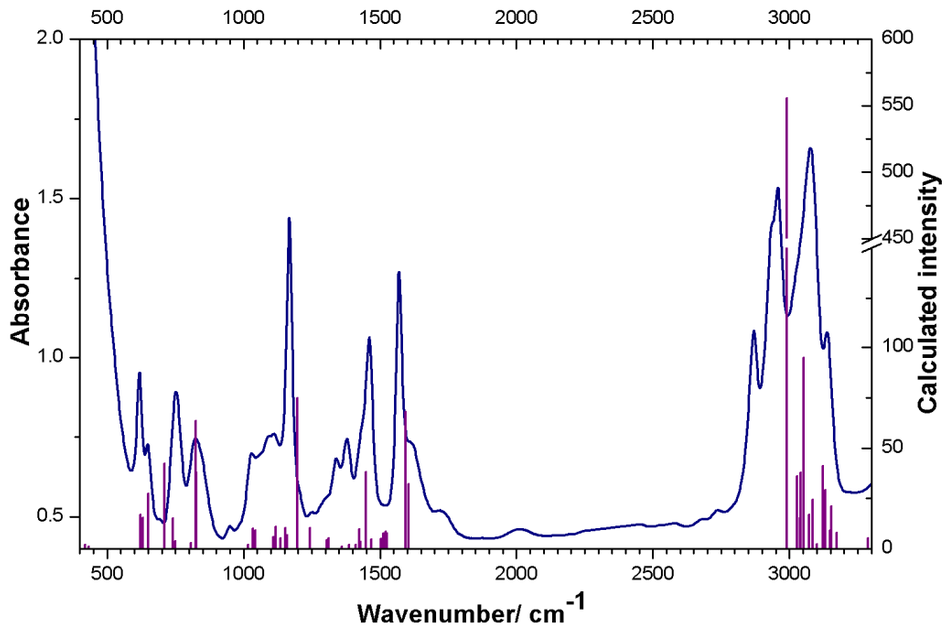

Fig. 6. Correlation of experimental and DFT calculated IR spectra of bmimI

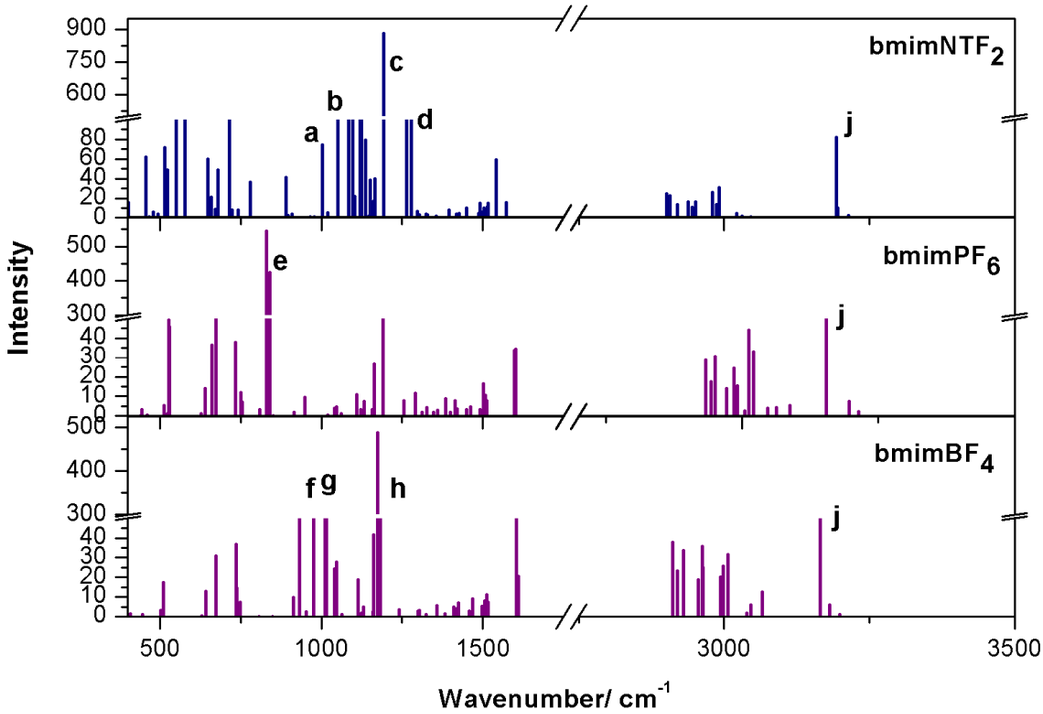

Fig. 7. DFT calculated IR spectra of bmimX where X=PF_6, BF_4 and NTf_2. Important bands have been marked. a, b, c, d bands are for C- S , C-F, N-S, S=O stretching respectively in bmimNTf_2. e band is for P-F stretching in PF_6 and f, g, h indicate in plane B-F stretching, and vertical B-F stretching in BF_4. Band marked as j indicates C_2-H stretch in all three ILs.

vibrational stretching frequency which is anharmonic in nature and the DFT calculated vibrational frequency which is harmonic in nature. Frequency of low wavenumber is found to match excellently while that of higher wavenumber deviated from theoretical values which are due to the increase in anharmonicity at higher wavenumber.

Hence a scaling factor of 0.9889 was used for all calculated values above 3000 cm^{-1}. The experimental results can be interpreted and rationalized in the light of theoretical investigations. Table 2 presents the assignments of different bands based on calculation. DFT calculated IR spectra for $bmimNTf_2$, $bmimPF_6$ and $bmimBF_4$ at B3LYP/6-31G++(d,p) level of calculation are shown in **Figure 7.** In $bmimNTf_2$ spectra S=O, N-S, C-F and C-S bond found to be at 1281 cm^{-1}, 1195 cm^{-1}, 1122 cm^{-1} and 1046cm^{-1}.[37] In $bmimPF_6$, P-F symmetric and asymmetric stretching found at 827 cm^{-1} and 841 cm^{-1} respectively. In $bmimBF_4$, B-F stretching (vertical) found at 1174 cm^{-1} and B-F stretching (in plane) found at 1009 cm^{-1} and 975 cm^{-1}. In higher wavenumber region intense peak found at 3373 cm^{-1}, 3233 cm^{-1} and 3278 cm^{-1} in $bmimNTf_2$, $bmimPF_6$ and $bmimBF_4$ respectively which is due to C_2-H stretching in imidazolium cation. Hence with variation of anion, C_2-H stretching frequency shift is observed. Experimental IR spectra of the $bmimNTf_2$, $bmimPF_6$ and $bmimBF_4$ ILs which we have synthesized have been correlated with the DFT calculated data and are shown in **Figure 8(a), 8(b) and 8(c)** respectively. To correlate well a scaling factor of 0.943, 0.975 and 0.965 has been applied in higher wavenumber region (above 3000cm^{-1}) for $bmimNTf_2$, $bmimPF_6$ and $bmimBF_4$ respectively. Hence the DFT calculated results found to be matching well with the experimental data.

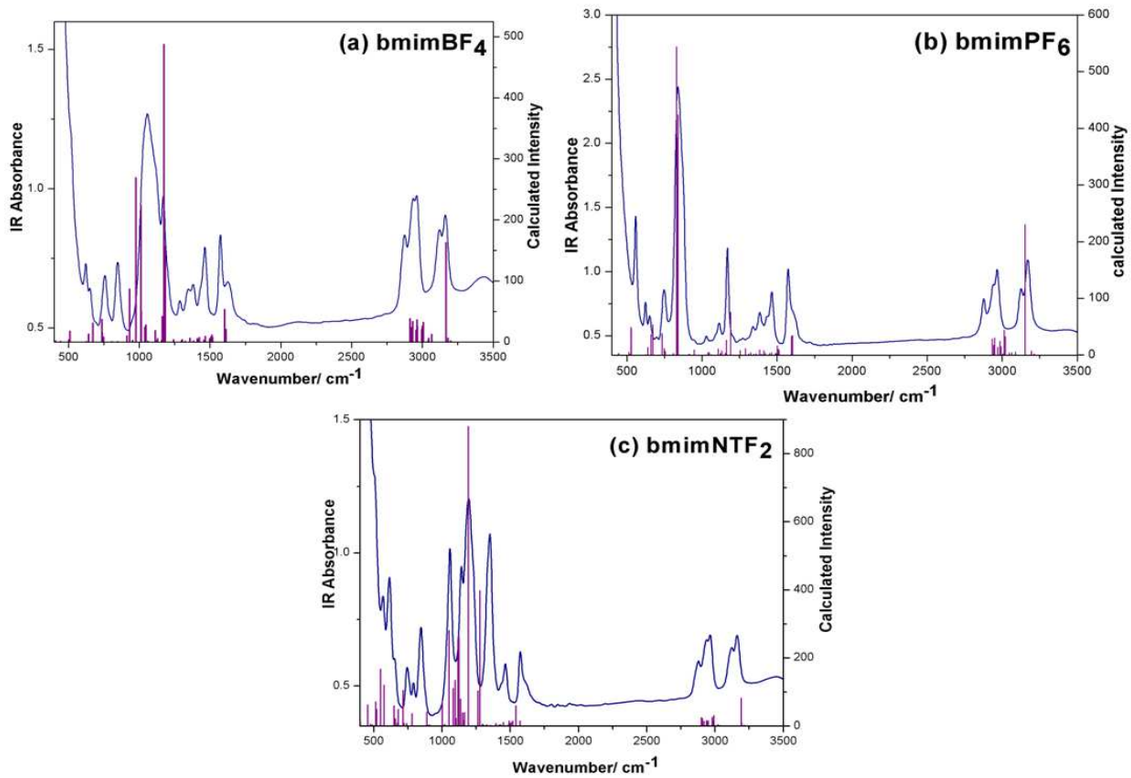

Fig. 8. (a). Experimental and DFT calculated IR spectra of (a) $bmimBF_4$. (b) $bmimPF_6$. (c) $bmimNTf_2$

As can be seen from the above figures, DFT can predict very well the vibrational bands of various ILs as discussed above. Therefore, assignment of experimental bands becomes a easy task, thereby helping us to understand completely the structure and interactions present in the ILs.

4.5 Transitions in bmimX: UV-Vis spectra and TD-DFT calculations

The UV-Visible spectrum of neat bmimCl and bmimBr could not recorded in absorbance mode, as they are solid at ambient temperature. The UV-Visible spectrum of pale yellow coloured bmimI was recorded and is presented in **Figure 9**.

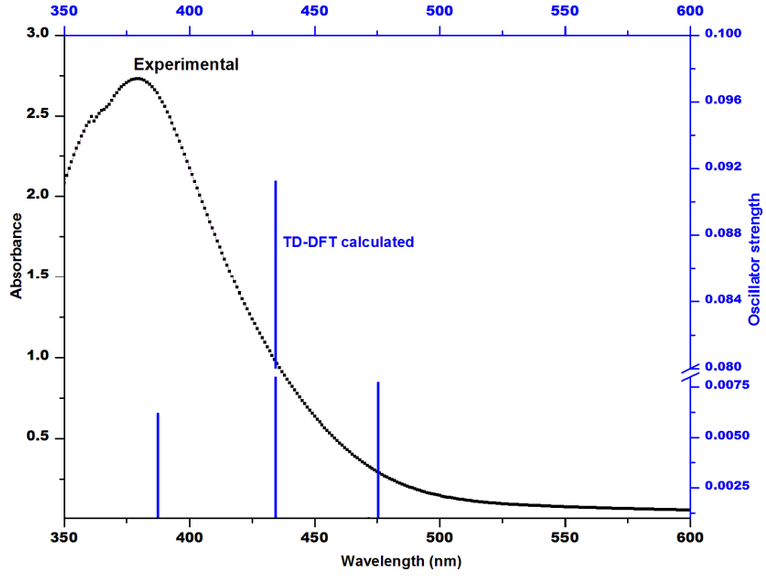

Fig. 9. UV-Vis spectrum (smooth line) of neat bmimI RTIL recorded using quartz cuvette having 5mm path length (Vertical lines correspond to calculated transitions using TD-DFT calculation))

While the peak of the spectrum appears at about 380 nm, long absorption tail is extended to about 525 nm. The interesting aspect is that the bmimI has pale yellow colour while the analogous derivatives of pure chloride and bromide are colourless. It is well known fact that during the process of synthesising these ILs, often colour impurity makes the resultant ILs coloured. In most of the cases improperly purified or unpurified ILs shows pale colour whereas on persistent and proper purifications, the final IL comes out to be colourless.[26, 38] So, to understand whether the bmimI is inherently pale yellow coloured or the colour is due to presence of impurity, time dependent DFT (B3LYP) calculations were performed on bmimCl, bmimBr and bmimI. For bmimCl and bmimBr, transitions found to occur below 356 nm (only in UV region), whereas in case of bmimI, transition found to occur in visible region also. The wavelengths of calculated transitions for bmimI, along with their oscillator strengths are presented in Figure 10. Even though the calculated oscillator strengths of various possible transitions do not exactly corresponds with that of experimentally observed spectrum (vide Figure 10), it does strongly indicate couple of transitions (though weak, at 371 and 380nm) in visible range.

The important point here to note is that a couple of transitions also occur at much longer wavelengths 434 and 475 nm having reasonably good oscillator strengths. Thus it is confirmed that the pale yellow colour of the bmimI is inherently due to the transition in bmimI itself.

Transition Wavelength (nm)	Transition occurring from one MO to other MO	Oscillator strength	Energy (eV)
475	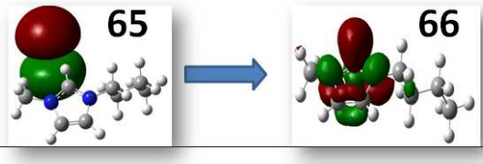	0.0027	2.6079
471	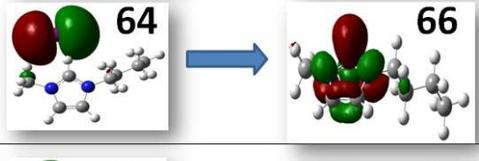	0.0002	2.6293
434	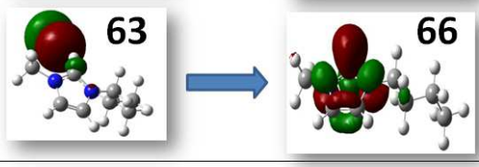	0.0912	2.8549
387	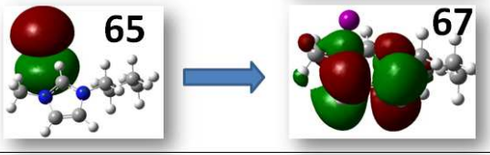	0.0017	3.2024
380	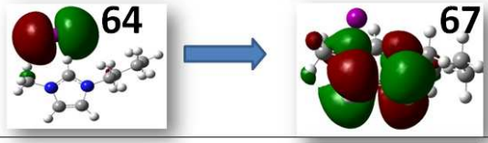	0.0011	3.2593
371	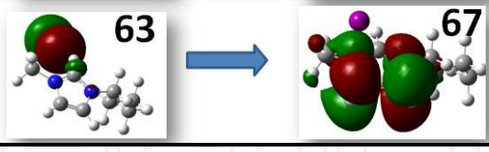	0.0008	3.3356

Fig. 10. Some important Frontier Molecular Orbitals of bmimI ion pair are shown which is obtained by calculation at B3LYP/DGDZVP level.

Being confirmed that the observed colour of bmimI is inherent to this IL, we have investigated the involvement of orbitals through Molecular Orbital (MO) analysis. **Figure 10** depicts the orbitals responsible for various low energy transitions. From this frontier molecular orbital pictures it is clear that HOMO is the non-bonding orbital localized on iodide ion (due to presence of lone pair electron) while LUMO is mainly localized on imidazolium ring and is antibonding in nature (π*). Thus the transition which is responsible for pale yellow colour of bmimI is due to charge transfer transition occurring from HOMO on iodide anion to LUMO on imidazolium cation. The strongest transition in the visible range (434nm) was found to be from MO 63 to MO 66 (shown in Figure 10) having oscillator strength of 0.0912.

Hence the pale yellow colour of bmimI is found to be intrinsic of this room temperature IL and is due to the charge transfer from iodide anion to imidazolium ring ($n \rightarrow \pi^*$). UV-visible spectra of bmimNTf2, bmimPF6 and bmimBF4 were also recorded and these ILs were found to be colourless liquids. Similar TD-DFT calculations for these RTILs are also done and supports the experimental observation. In all of these RTILs, as shown in Figure 11 (a-c) transitions found to occur in UV region only, that is why, they are transparent in visible region.

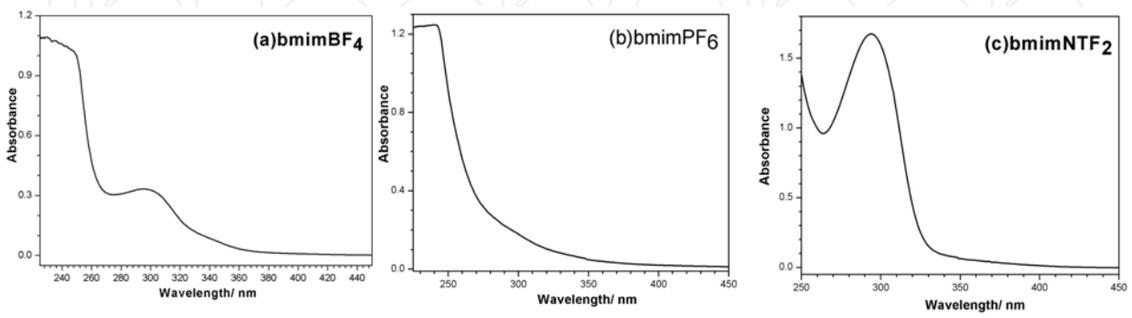

Fig. 11. UV-Visible spectra of (a) $bmimBF_4$,(b) $bmimPF_6$ and (c) $bmimNTf_2$. Quartz cuvette with 1cm path length was used for all the measurements.

Because of their clear optical window, these RTILs have extensively been used as a medium for photophysical studies of various probe molecules and solvation dynamics in recent years. [30, 39-41]

5. Conclusion

Modified synthesis of different imidazolium based ILs having simple mono atomic to complex anions have been described here. In addition to usual characterizations, ^{1}HNMR spectra are used to extract information on existence and strength of H-bondings present in the ILs having the mono-atomic anion. IR spectroscopy has extensively been used to analyse the interaction present in the ILs. A through DFT calculation at B3LYP level have been performed on the all the ILs to get fully optimized geometry and obtained complete vibrational spectra. These calculations help us to understand the structure and existence of various interactions including H-bonding interactions. Monoatomic anion based ILs (bmimCl, bmimBr and bmimI) found to have only one predominant H-bonding between cation and anion through C_2-H while multiple H-bonding interactions were found to exist in $bmimNTf_2$, $bmimPF_6$ and $bmimBF_4$ ILs. TD-DFT calculations were also presented to understand and interpret the experimental UV-Visible spectra of various ILs. That iodide ILs have pale yellow color while corresponding chloride and bromide ILs are colorless can well be explained with the TD-DFT calculations.

6. Acknowledgement

Financial assistance from CSIR, India (01(2210)/08/EMR-II) and DST, India (SR/FTP/CS-70/2006) are gratefully acknowledged. MLS and NS thanks UGC and CSIR respectively for fellowships. SS thanks Banaras Hindu University for providing the infrastructure and facilities.

7. References

[1] Plechkova, N. V. & Seddon, K. R., (2008) *Chem. Soc. Rev. Vol. 37*, pp. 123.
[2] Samanta, A., (2010). *J. Phys. Chem. Lett., Vol. 1*, pp. 1557.
[3] Saha, S. & Hamaguchi, H., (2006) *J. Phys. Chem. B. Vol. 110*, pp. 2777.
[4] Saha, S., Hayashi, S., Kobayashi, A. & Hamaguchi, H., (2003) *Chem. Lett. Vol. 32*, pp. 740.
[5] Zhao, H. & Malhotra, S. V., (2002) *Aldrichimica Acta Vol. 35*, pp. 75.
[6] Docherty, K. M., Dixon, J. K. & Kulpa, C. F. Jr (2007) *Biodegradation 18*, pp. 481.
[7] Zhang, C., Wang, H., Malhotra, S. V., Dodge, C. J. & Francis, A. J., (2010) *Green Chem., Vol. 12*, pp. 851.
[8] Domańska, U., (2010) *Int. J. Mol. Sci., Vol. 11*, pp. 1825
[9] Cadena, C., Zhao, Q., Snurr, R. Q., & Maginn, E. J., (2006) *J. Phys. Chem. B, Vol. 110,* pp. 2821.
[10] Kunze, M., Jeong, S., Paillard, E., Winter, M., & Passerini, S., (2010) *J. Phys. Chem. C, Vol. 114,* pp. 12364.
[11] Johansson, P., Fast, L. E., Matic, A., Appetecchi, G. B. & Passerini, S., (2010) *J. Power Sources Vol. 195,* pp. 2074 .
[12] Santos, C. S., Murthy, N. S., Baker, G. A., & Castner, E. W., Jr. (2011) *J. Chem. Phys. Vol.* 134, pp.121101-1
[13] Erdmenger, T., Vitz, J., Wiesbrock, F. & Schubert, U. S., (2008) *J. Mater. Chem., Vol. 18*, pp. 5267.
[14] Emelyanenko, V. N., Verevkin, S. P. & Heintz, A., (2009) *J. Phys. Chem. B, Vol. 113.* pp. 9871
[15] Fredlake, C. P., Crosthwaite, J. M., Hert, D. G., Aki, S. N. V. K. & Brennecke, J. F., (2004) *J. Chem. Eng. Data, Vol. 49*, pp 954.
[16] Anderson, J. L., Ding, J., Welton, T. & Armstrong, D. W., (2002) *J. Am. Chem. Soc., Vol. 124*, pp 14247.
[17] Logotheti, G. E., Ramos, J., & Economou, I. G., (2009) *J. Phys. Chem. B Vol. 113*, pp. 7211.
[18] Talaty, E. R., Raja, S., Storhaug, V. J., Dolle, A., & Carper, W. R. (2004) *J. Phys. Chem. B Vol. 108*, pp. 13177.
[19] Dong, K., Zhang, S., Wang, D. & Yao, X. (2006) *J. Phys. Chem. A, Vol. 110,* pp. 9775.
[20] Danten, Y., Cabaco, M. I. & Besnard, M., (2009) J. *Phys. Chem. A, Vol. 113,* pp. 2873
[21] Ozawa, R., Hayashi, S., Saha, S., Kobayashi, A., & Hamaguchi, H., (2003) *Chem. Lett. Vol.* 32, pp. 948.
[22] Hamaguchi, H. & Ozawa, R., (2005) *in Adv. Chem. Phys. Vol.* 131, pp. 85.
[23] Shukla, M., Srivastava, N. & Saha, S., (2010) *J. Mol. Struc. Vol.* 975, pp. 349.
[24] Chang, H. C., Jiang, J. C., Chang, C. Y., Su, J. C., Hung, C. H., Liou, Y. C. & Lin, S. H., (2008) *J. Phys. Chem. B, Vol. 112*, pp 4351.
[25] Seddon, K. R., (2003) *Nature mater., Vol. 2*, pp 363.
[26] Srivastava, N., Shukla, M. & Saha, S., (2010) *Ind. J. Chem. Vol. 49A*, pp. 757.
[27] Turner, E. A., Pye, C. C. & Singer, R. D., (2003) *J. Phys. Chem. A, Vol. 107*, pp 2277.
[28] Paul, A., Mandal, P. K., & Samanta, A., (2005) *J. Phy. Chem. B Vol. 109*, pp. 9148.
[29] Samanta, A., (2006) *J. Phys. Chem. B Vol.* 110, pp. 13704.
[30] Saha, S., Mandal, P. K., & Samanta, A., (2004) *Phys. Chem. Chem. Phys. Vol.* 6, pp. 3106.
[31] Holbrey, J. D., Reichert, W. M., Nieuwenhyuzen, M., Johnston, S., Seddon, K. R., Rogers, R. D., (2003) Chem. Commun., pp.1636,

[32] Frisch, M. J.; Trucks, G. W.; Schlegel, H. B.; Scuseria, G. E.; Robb, M. A.; Cheeseman, J. R.; Montgomery Jr., J. A.; Vreven, T.; Kudin, K. N.; Burant, J. C.; Millam, J. M.; Iyengar, S. S.; Tomasi, J.; Barone, V.; Mennucci, B.; Cossi, M.; Scalmani, G.; Rega, N.; Petersson, G. A.; Nakatsuji, H.; Hada, M.; Ehara, M.; Toyota, K.; Fukuda, R.; Hasegawa, J.; Ishida, M.; Nakajima, T.; Honda, Y.; Kitao, O.; Nakai, H.; Klene, M.; Li, X.; Knox, J. E.; Hratchian, H. P.; Cross, J. B.; Bakken, V.; Adamo, C.; Jaramillo, J.; Gomperts, R.; Stratmann, R. E.; Yazyev, O.; Austin, A. J.; Cammi, R.; Pomelli, C.; Ochterski, J. W.; Ayala, P. Y.; Morokuma, K.; Voth, G. A.; Salvador, P.; Dannenberg, J. J.; Zakrzewski, V. G.; Dapprich, S.; Daniels, A. D.; Strain, M. C.; Farkas, O.; Malick, D. K.; Rabuck, A. D.; Raghavachari, K.; Foresman, J. B.; Ortiz, J. V.; Cui, Q.; Baboul, A. G.; Clifford, S.; Cioslowski, J.; Stefanov, B. B.; Liu, G.; Liashenko, A.; Piskorz, P.; Komaromi, I.; Martin, R. L.; Fox, D. J.; Keith, T.; Al-Laham, M. A.; Peng, C. Y.; Nanayakkara, A.; Challacombe, M.; Gill, P. M. W.; Johnson, B.; Chen, W.; Wong, M. W.; Gonzalez, C.; & Pople, J. A. *Gaussian, Inc.*:, Wallingford, CT, 2004.
[33] Becke, A. D., (1993) *J. Chem. Phys. Vol.* 98, pp. 5648.
[34] Tsuzuki, S., Katoh, R., & Mikami, M., (2008) *Mol. Phys. Vol. 106*, pp. 1621.
[35] S. Tsuzuki, A. A. Arai, and K. Nishikawa, (2008) *J. Phys. Chem. B*, *Vol. 112*, 7739.
[36] V. Kempter, B. Kirchner, (2010) *J. Mol. Struc.*, doi:10.1016/j.molstruc.2010.02.003.
[37] Fujii, K., Seki, S., Fukuda, S., Kanzaki, R., Takamuku, T., Umebayashi, Y. & Ishiguro, S. (2007) *J. Phys. Chem. B Vol. 111*, pp. 12829.
[38] Stark, A., Behrend, P., Braun, o., Muller, A., Ranke, J., Ondruschka, B. & Jastorff, B. (2008) Green Chem. *Vol. 10*, pp 1152.
[39] Kanaparthi, R.K., Sarkar, M. & Samanta, A., (2009) *J. Phys. Chem. B Vol. 113,* pp. 15189.
[40] Santhosh, K. & Samanta, A., (2010) *J. Phys. Chem. B Vol. 114,* pp. 9195.
[41] Samanta, A., (2010) *J. Phys. Chem. Lett. Vol. 1*, pp. 1557.

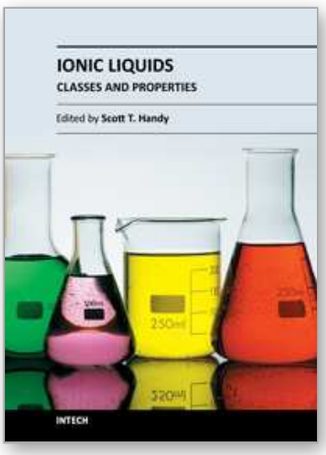

Ionic Liquids - Classes and Properties

Edited by Prof. Scott Handy

ISBN 978-953-307-634-8
Hard cover, 344 pages
Publisher InTech
Published online 10, October, 2011
Published in print edition October, 2011

Room temperature ionic liquids (RTILs) are an interesting and valuable family of compounds. Although they are all salts, their components can vary considerably, including imidazolium, pyridinium, ammonium, phosphonium, thiazolium, and triazolium cations. In general, these cations have been combined with weakly coordinating anions. Common examples include tetrafluoroborate, hexafluorophosphate, triflate, triflimide, and dicyanimide. The list of possible anionic components continues to grow at a rapid rate. Besides exploring new anionic and cation components, another active and important area of research is the determinination and prediction of their physical properties, particularly since their unusual and tunable properties are so often mentioned as being one of the key advantages of RTILs over conventional solvents. Despite impressive progress, much work remains before the true power of RTILs as designer solvents (i.e. predictable selection of a particular RTIL for any given application) can be effectively harnessed.

How to reference

In order to correctly reference this scholarly work, feel free to copy and paste the following:

Madhulata Shukla, Nitin Srivastava and Satyen Saha (2011). Interactions and Transitions in Imidazolium Cation Based Ionic Liquids, Ionic Liquids - Classes and Properties, Prof. Scott Handy (Ed.), ISBN: 978-953-307-634-8, InTech, Available from: http://www.intechopen.com/books/ionic-liquids-classes-and-properties/interactions-and-transitions-in-imidazolium-cation-based-ionic-liquids

INTECH
open science | open minds

InTech Europe
University Campus STeP Ri
Slavka Krautzeka 83/A
51000 Rijeka, Croatia
Phone: +385 (51) 770 447
Fax: +385 (51) 686 166
www.intechopen.com

InTech China
Unit 405, Office Block, Hotel Equatorial Shanghai
No.65, Yan An Road (West), Shanghai, 200040, China
中国上海市延安西路65号上海国际贵都大饭店办公楼405单元
Phone: +86-21-62489820
Fax: +86-21-62489821

IntechOpen